Adaptive Single Pole Automatic Reclosure for Compensated Transmission Systems

Ahmed R. Adly[1*], Ragab A. El Sehiemy[2], Mahmoud A. Elsadd[3], Almoataz Y. Abdelaziz[4]

[1] Nuclear Research Center, Atomic Energy Authority, Egypt
[2] Faculty of Engineering, Kafrelsheikh University, Egypt
[3] Faculty of Engineering, Menoufia University, Egypt
[4] Faculty of Engineering, Ain Shams University, Egypt
[*]ahmed.adly@eaea.org.eg

Abstract: Adaptive single pole automatic reclosure (ASPAR) scheme for transmission lines (TL) using wavelet packet transform (WPT) is presented in this paper. The presented scheme only needs on-line voltage data that are sampled from one end of the lines. The proposed scheme uses an adaptive threshold level in order to be suitable for the probable network-topology changes. The scheme is based on second, third, and fifth harmonics values in order to distinguish between the permanent and temporary (transient) faults. Also, it is based on monitoring the DC component to identify the arc extinction time. The performance evaluation is accomplished considering 220 kV single and double circuits transmission lines, simulated by the ATP/EMTP package under different system configurations such as shunt/series compensators (shunt reactors and series capacitors). The impact of shunt/series compensators on the line voltage is noticed and, therefore, the mal-operation of the presented auto-reclosing scheme is avoided. The sample results of the assessment are declared and discussed.

Keywords– Adaptive single pole autoreclosure, Wavelet packets transform, Temporary fault, Permanent fault.

1. Introduction

Fast and accurate fault detection in transmission networks affect restoration of power supply and improve the reliability [1]. Network reliability can be improved by a successful decision of an automatic reclosing to a line. When applying single phase tripping schemes, a number of issues are necessary to be considered such as automatic reclosing and pole disagreement [2]. Adaptive auto reclosing recloses due to temporary faults and avoids reclosing due to permanent faults. Conventional single pole automatic reclosure schemes reconnect the faulted phase after a definite dead time irrespective of fault circumstances. Specified interval dead time can reflect the time margin for a phase to separate from the three phase line keeping on system stability. Reducing the dead time increases the margin of stability [3].

Reference [4] reviewed different wavelet transform algorithms for fault identification in TL for enhancing adaptive single pole tripping schemes. In [5], the authors presented ASPAR based on the zero-sequence power from both ends of a TL to detect the instant of arc extinction. In [6], the authors presented ASPAR based on the third harmonic of the faulted phase voltage. In [7], the RMS value of the faulty phase voltage waveform has been utilized to detect the final arc extinction time. In [8], an algorithm was proposed for ASPAR. The algorithm distinguishes between the fault's nature based on the DC offset value of the zero-sequence voltage. In [9], a scheme that is dependent on the transmission line voltage and current phasors at both terminals was presented. It calculates total harmonic distortion (THD) and compares it with a fixed threshold. The schemes in [10] and [11] presented a WPT-based approach and employed the db8 to decompose the decision signal. In [12], a method based on WPT is presented for discrimination between permanent and temporary faults. The algorithm in [13] was dependent on the third harmonic component and fundamental component of the faulty phase voltage based on discrete Fourier transform.

In [14], the voltage and current phasors at line terminals were used to calculate total harmonic distortion (THD) and compared it with a fixed threshold. In [15], a method dependent on tracking a single harmonic distortion index (HDI) using DFT was presented to represent the behaviour of the low-frequency components of the faulty phase voltage or sound phase current. If the tracked HDI moves beyond a fixed threshold, then the fault is temporary. In [16], a method based on local voltage magnitude, and the faulty phase angle was presented. The presented method is able to fastly distinguish the fault type and the arc extinction if the fault is transient.

In [17] and [18], simple techniques are presented based on the wavelet packet transform (WPT). The db6 is treated as a mother wavelet to decompose the faulted phase voltage. In [19], the suggested scheme is based on extracting the first and third harmonics from faulty phase voltage and used them as input data for ANN to distinguish between the permanent and temporary faults.

The salient challenges of ASPAR can be summarized as:

- Transmission line has been equipped with fourth leg neutral reactor to reduce the time of the arc extinguish under temporary fault. However, after the installation of fourth leg neutral reactor, the parameters of the electrical system will be changed, also the recovery voltage and arc current will be increased. Therefore, some ASPAR schemes find limitations as in [7], [8], [10] and [11].
- Transmission line has been equipped with series capacitors to enhance transmission capacity. However, after the installation of series capacitors in high voltage transmission line, the line reactance variation and the sub-harmonic frequency oscillations may seriously

affect successful reclosing. References [5]-[19] do not consider the suppression effect of series capacitors.

- The causes of faults and their factors have great effects on the actual waveforms. The fault causes/factors involve source parameters, construction of the line, pre-fault loading, fault position and robustness to noise. It may delay arriving at a decision in several techniques, which are dependent on DFT as a signal processing tool [5]-[9], and may produce erroneous results. In this paper, authors use WPT as a signal processing tool. WPT is robust in extracting the noise, and it is more suitable compared to the familiar DFT method for non-stationary signal from the viewpoint of extracting the noise.
- The schemes mentioned in [12] and [13] utilized high frequency voltage and have the following limitations: difficulty in determining the temporary energies and spectral of a system, where they require special design transducers with high-frequency temporary-voltage detectors.
- Training and huge samples are needed. The technique in [19] needs training for learning representation and uses high number of samples, leading to a complicated job. Also, these techniques may not manage the undecided factors in the transmission networks. In this paper, authors do not depend on any intelligent classifier to form a simple identification criterion.
- The limitations of fixed-threshold value for fault identification schemes in power transmission systems (with any modification in configuration of power transmission systems, a new threshold must be determined).

The main contribution of this paper is presenting a new adaptive single pole automatic reclosure suitable for the probable network-topology change via updating the threshold value. The proposed scheme is based on only monitoring the measured voltage at single end in order to identify both the fault type and the arc extinction instant of the secondary arc. This identification is, respectively, conducted via monitoring the second, third, and fifth harmonics and the DC component using WPT. WPT is used for harmonic extraction tools. WT could be a tool or function that cuts up information to completely different frequency elements, then uses every element with a resolution matched to its scale. WT is ready to reveal signal aspects that different analysis techniques loss, as an example trends, discontinuities, etc. The waveform decomposition results from discrete wavelet transform (DWT) provide non-uniform frequency bands. The DWT algorithm is developed to the WPT. In WPT, the details as well as the approximations can be divided. The merits of the WPT are that, it can decompose a waveform into uniform frequency bands [20].

2. Description of Proposed Fault Identification Scheme

The arcing characteristic of faults leads to distortions of the arc voltage. Investigating the faulty phase voltage harmonics, it is noticed that the magnitudes of the second, the third and the fifth harmonics (Nodes 3, 4, 5, 6, 9 and 10) are higher than that of the rest of the harmonics. Thus, the proposed scheme utilizes the magnitude of these harmonics as the most parameter for a reliable energy coefficient index (S_a) for distinguishing between faults types. After clearing the temporary fault, the secondary arc starts. As the recovery voltage is fully asymmetrical, thus the DC component is the most suitable parameter for identification of the extinction instant of the secondary arc as a result to inhomogeneous part of the faulted phase voltage founded at the instants of the maximum/minimum of the arc extinction time. Consequently, the proposed scheme utilizes the DC component's amplitude (Node 0) of the faulty phase as the most parameter for a reliable index for identification of the instant of the secondary arc extinction. The main issue of this scheme is the calculation of a preselected setting value (S_{th}) for successful discrimination between the fault natures that obtained in the following section. The S_{th} value determined prior the fault occurrence is utilized for that target. After tripping the faulty phase, the threshold magnitude is activated from the calculated S_a value during the healthy operation that is recorded in a shift registers. The flow chart of the presented scheme is illustrated in Figure. 1 and it will be briefly described as in the following steps:

- A Wavelet Packet Transform algorithm is employed to obtain proposed energy coefficients at a sampling rate of 6.4 kHz.
- The measured voltage signal is decomposed via db6 wavelet into level 7 to estimate the presented energy coefficients of the 7 nodes at various frequency extent as: Node 0 (the frequency range 0– 25 Hz), Node 3 (the frequency range 75–100 Hz), Node 4 (the frequency range 100–125 Hz), Node 5 (the frequency range 125–150 Hz), Node 6 (the frequency range 150–175 Hz), Node 9 (the frequency range 225–250 Hz), and Node 10 (the frequency range 250–275 Hz)
- Computing both the energy coefficient index (S_a) for distinguishing between fault natures and the energy coefficient index (S_d) and then normalizing it to determine the instant of extinguishing the arc. Thus, the energy coefficient indices are estimated as;

$$S_d = \sum_{i=1}^{N} d_0^2(i) \tag{1}$$

$$S_a = \sum_{i=1}^{N} \sum_{\substack{k=3,\\ k\neq 7,8}}^{10} d_k^2(i) \tag{2}$$

where d_k and N are the coefficients and the coefficients' number at node k, respectively. S_a, S_d are the energy indices.

After the circuit breakers are opened, the comparison between the esitimated S_a value and the threshold value will start and still during three cycles (D). If the threshold value (S_{th}) is more than the S_a, the type of the fault is permanent. The criteria for the proposed scheme to initiate a trip signal to the circuit breakers associated with the sound phases are achieved when the counter "WI" equals three cycles' samples (D). If S_a is greater than the threshold value (S_{th}) and the counter "FI" equals three cycles' samples (D), the fault type is temporary. Whenever the estimated S_d is greater than zero value, this means that arc is extinguished.

This paper selected the most suitable mother wavelet for this target by extensive studies to be db6 as the mother wavelet [20].

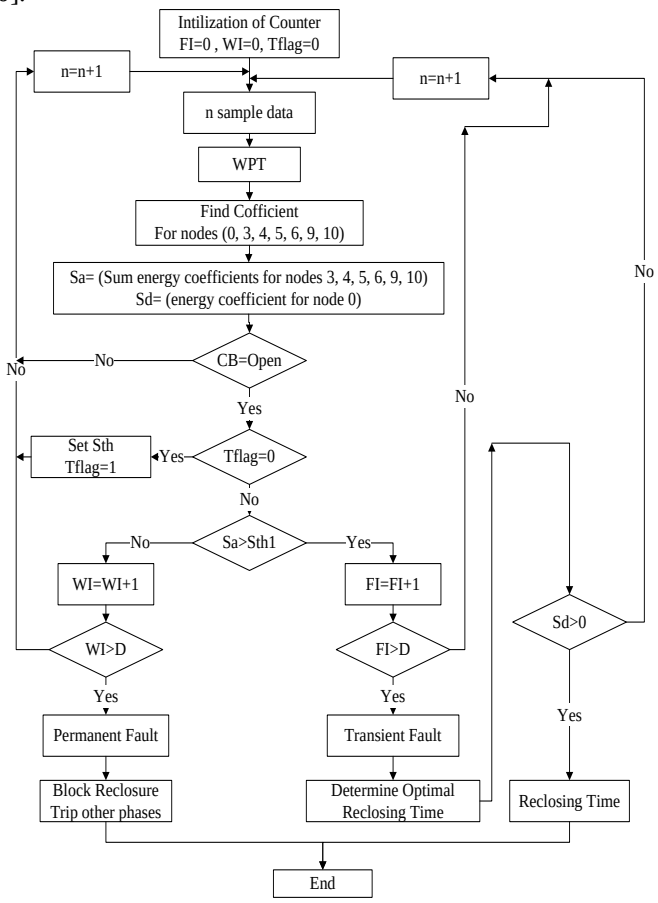

Fig. 1. *Flow chart of the proposed scheme*

3. Simulation and Discussion

3.1. Test System

Typical systems, including transmission lines shown in Figure 2 and the arc fault are conducted utilizing ATP/EMTP. The ATP/EMTP created different cases which are then loaded into MATLAB. The main parameters of a single circuit shunt compensated line as shown in Figure 2(a) are given as demonstrated in [21]. Figure 2(b) shows single circuit with series compensated by series capacitors jointed at the midline with compensation rate equal to 70%. Also a double circuit network as shown in Figure 2(c) with mutual coupling is considered for testing the proposed scheme under different network configurations. The main parameters of the double circuit network are demonstrated in [22].

In this paper, ATP/EMTP was employed for modelling the secondary arc. The arc is modelled by a MODELS controlled switch and a controlled resistance in ATP. Equation (3) is used to model the secondary and primary arcs [23] as:

$$\frac{dg}{dt} = \frac{1}{\tau}(G - g) \qquad (3)$$

where, τ is the constant arc time, G is the stationary conductance arc and g is the arc conductance varying time. Using the thermal arc model of [23], the conductance stationary arc is calculated as:

$$G = \frac{|i|}{(U_0 + R|i|)l} \qquad (4)$$

where, i is the arc current, U_0 is the arc voltage drop per unit length, l is the arc length, and R is the total arc resistance.

For the primary arc τ and l are equal and constant to initial values τ_0 and l_o, where τ and l for the secondary arc will change with time. The variation of the length of the arc is dependent on the wind velocity. This change can be approximated by (5) for relatively low wind velocities from 0 to 1 m/s.

$$l = \begin{cases} 10 t_r l_o \longrightarrow t > 0.1s \\ l_o \longrightarrow t \le 0.1s \end{cases} \qquad (5)$$

where, t_r is the initiation time of the secondary arc and l_o is the initial length of the arc. The τ can be defined as:

$$\tau = \tau_0 \left(\frac{l}{l_0} \right)^{\alpha} \qquad (6)$$

where, α is the negative value coefficient.

For tested networks, a proper arc model (Arc1, Arc2, Arc3) is used. Table 1 show three parameters varied to generate three different arcs. Validation of the arc modelling technique is done by comparing the modelled arc with other simulations and real arc waveforms [24].

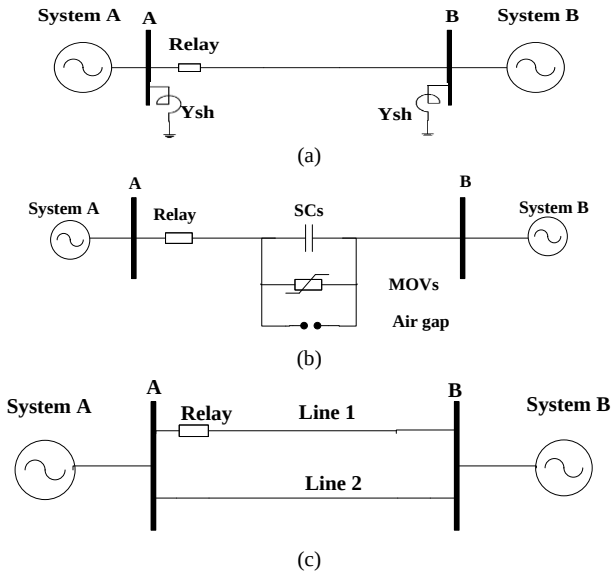

Fig. 2. *Tested systems*
(a) Single circuit with shunt reactors, (b) Single circuit with series capacitors, (c) Double circuit line

Table 1 Different arcs parameters

	λ0(ms)	u0(v/cm)	L0(m)
Arc1	0.714	12	3.5
Arc2	0.555	8	3.15
Arc3	0.833	11	3.5

3.2. Studies Cases

Numerous simulation tests have been employed to confirm the validity of the presented scheme under various

fault situations. The studied cases to verify the proposed technique can be classified in the following six cases:

Case 1: Single circuit with shunt compensated line.
Case 2: Single circuit with series compensated line.
Case 3: Double circuit line.
Case 4: Single circuit line under different arc models (Arc1, Arc2, Arc3).
Case 5: Effect of sampling frequency on the scheme.
Case 6: Comparison with the schemes described in [5] and [7] based on time delay.

3.3. Analysis of permanent & temporary faults.

Case 1, in the case of compensated TL via installing a shunt reactor, the residual voltage of the faulted phase consists of the frequency oscillation component due to the residual voltage coupled from both the sound phases. Therefore, the residual voltage compound on the faulted phase will appear as a swing behavior as shown in Figure 3 with high closeness to the analysis presented in [25]. Figure 3 illustrates the system primary voltages for the permanent and temporary AG faults at the sending end for case 1 where the fault occurred at t1. Following changing the arc from primary to secondary at t2, followed by the gradual raise of arc path voltage until extinguishing arc takes place at t3. For temporary faults, a typical characteristic wave shape can be ascertained on the faulty phase voltage attributable to the secondary arc. The voltage wave shape of the faulty phase during temporary faults includes voltage distortions. After just clearing the temporary fault, there still remains a little voltage, referred to as recovery voltage.

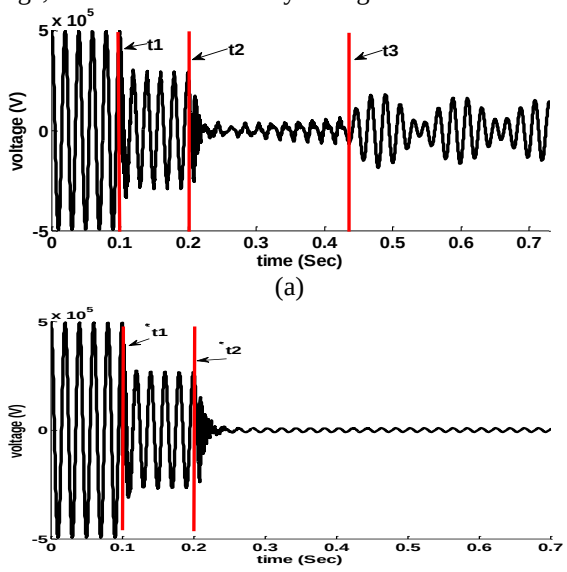

Fig. 3. *Primary system voltages for cases 1 at 175 km from sending end for a typical 'AG' to earth fault.*
(a) Temporary fault, **(b)** Permanent fault

Figure 4 shows the system primary voltages under the permanent and the temporary AG faults recorded at the sending end for case 2 which occurred at t1. Also how the series compensation capacitors affect the faulty phase voltage under temporary fault and leading to more harmonics because the series capacitors generate high frequency transients and sub-harmonic frequency oscillations under fault. Figure 5 shows the system primary voltages under the permanent and the temporary AG faults at the sending end for different network configurations (double circuit) case 3.

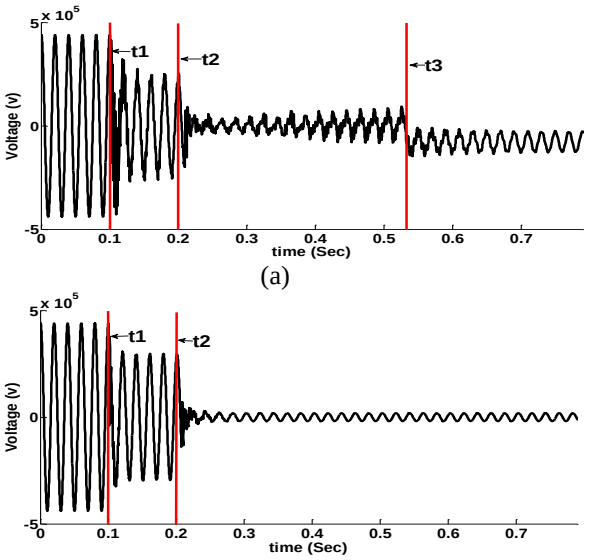

Fig. 4. *Primary system voltages for cases 2 at 175 km from sending end for a typical 'AG' to earth fault.*
(a) Temporary fault, **(b)** Permanent fault

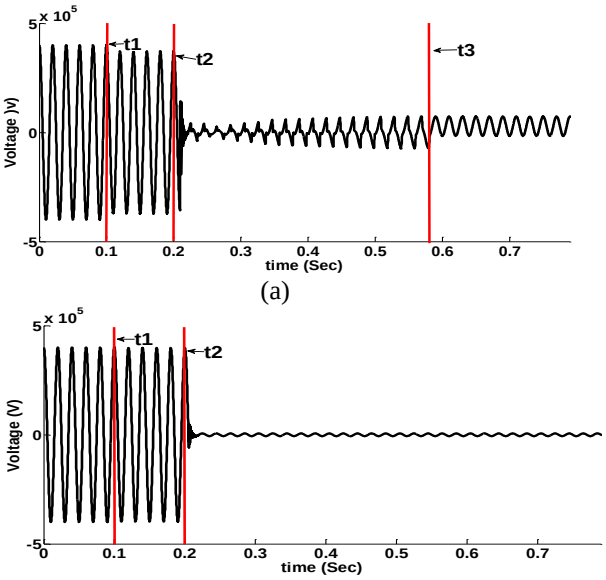

Fig. 5. *Primary system voltages for cases 3 at 50 km from sending end for a typical 'AG' to earth fault.*
(a) Temporary fault, **(b)** Permanent fault

3.4. Response of fault identification scheme

Several test cases, corresponding to the analyzed case 1, have been taken into consideration in this section for checking the presented technique ability in order to properly distinguish among the temporary and permanent faults. This is shown by simulation tests performed for the case where the transmission line is shunt compensated. Figures 6(a) and 6(b) illustrates the counterpart response of the presented technique for case 1 at different locations. In all cases, the fault occurred at t1 (80 ms) and the circuit breaker for the

faulted phase opening at t2 (180 ms). The temporary faults are obviously distinguished where the presented index value remains above the threshold value (S_{th}) under only these faults.

Also, figures 6(c) and 6(d) traced the behaviour of the proposed index (S_d) at different locations for Case 1. It can be seen from the figure that the detection time of secondary arc extinction is just when the index S_d has a value and this is done in time less than half cycle (10ms).

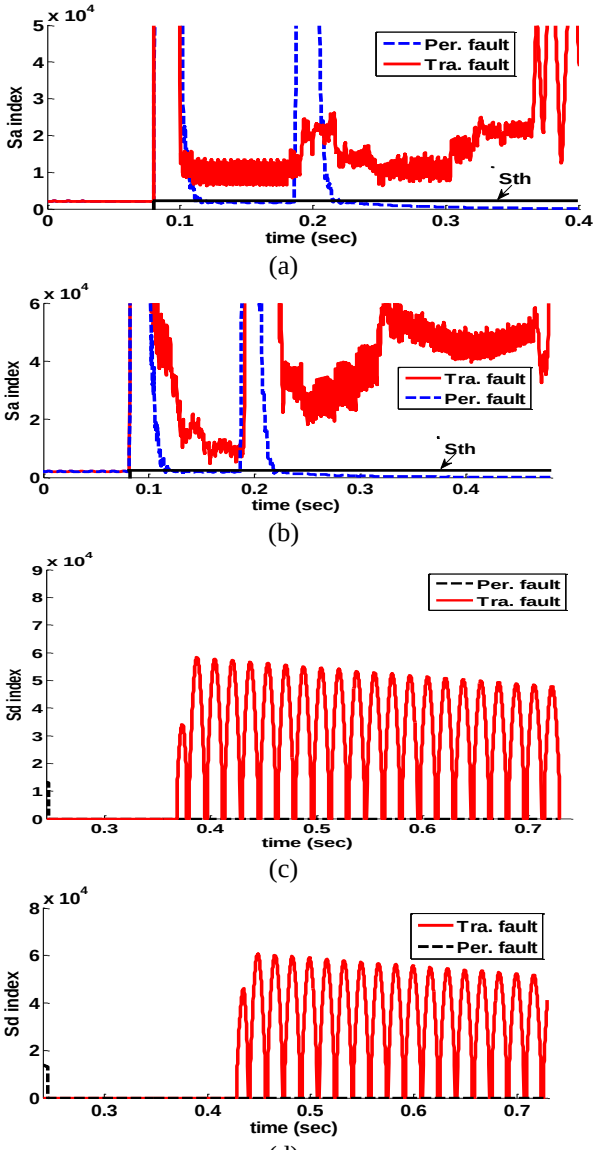

Fig. 6. *Behaviour of indices "S_a& S_d" under transient and permanent faults case 1 at different fault locations*
(a) S_a at 40 km, **(b)** S_a at 310 km, **(c)** S_d at 40 km, **(d)** S_d at 310 km

Case 2 has been considered for checking the presented technique ability for single circuit with series capacitors where AG fault occurs at instant 0.08 s. Figure 7 illustrates the counterpart response of the presented technique for single circuit series compensated line under different fault locations. Figures 7(c) and 7(d) show how the series capacitors affect to the secondary extinction time. Therefore, the insertion of series capacitors does not affect on the decision of the arc extinction of the proposed scheme. By considering the accuracy for detection of the secondary arc extinction, the presented scheme can be successfully implemented as a practical scheme.

Case 3 has been considered to realize the ability of the proposed scheme for double circuit line where AG fault occurs in line 1 at instant 0.08 s. Figure 8 illustrates the counterpart response of the presented technique for double circuit line under different fault locations for case 3. As obviously shown, indices learn the voltage waveform successfully. The sharp increase in the value of index (S_d) can be utilized to detect the arc extinction instant.

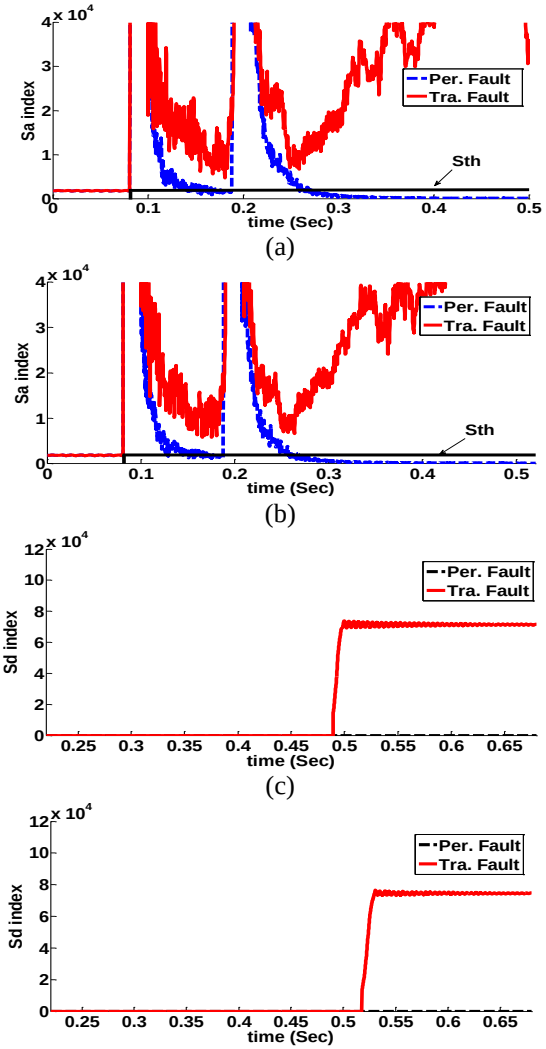

Fig. 7. *Behaviour of indices "S_a& S_d" under transient and permanent faults case 2*
(a) 150km (before Xc), **(b)** 150 Km (after Xc), **(c)** 150km (before Xc), **(d)** 150 Km (after Xc)

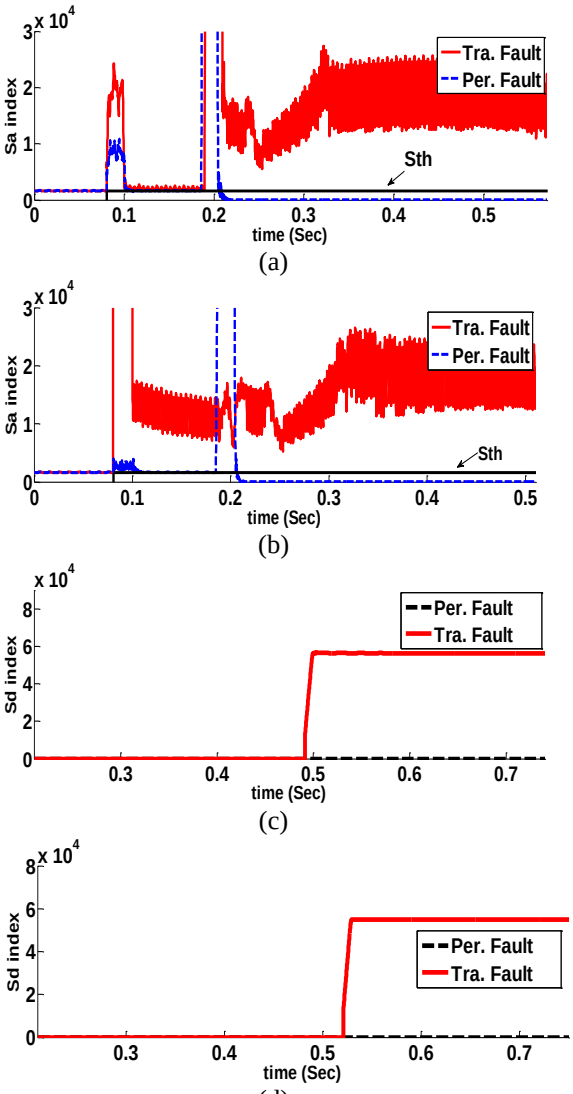

Fig. 8. *Behavior of indices "Sa" & "Sd" under transient and permanent faults for Case 3 at different fault locations*
(a) S_a at 20 km, **(b)** S_a at 90 km, **(c)** S_d at 20 km, **(d)** S_d at 90 km

Case 4 has been tested in this section for checking the presented scheme ability in order to properly distinguish among the faults natures with three different arc models (Arc1, Arc2, and Arc3). Figure 9 shows the counterpart signals captured for case 6 by tracing the behaviour of the proposed index (Sa) for temporary and permanent faults at different arc models. As obviously shown, the proposed index value stays greater than the threshold level (Sth) under temporary faults only and that ensures correct discrimination compared to the permanent fault.

Case 5 presents the effect of sampling frequency on the behaviour of the presented scheme. The sampling frequency used is set as f_s = 6.4 kHz (i.e., 128 samples /cycle at 50Hz), which means that the maximum resolution level that can be reached is the 7th level by WPT, i.e. 2N= 128 =27. In this paper, the proposed scheme is tested under similar condition with f_s = 3.2 kHz. A line-to-ground (AG) temporary fault type is created as in case 1.

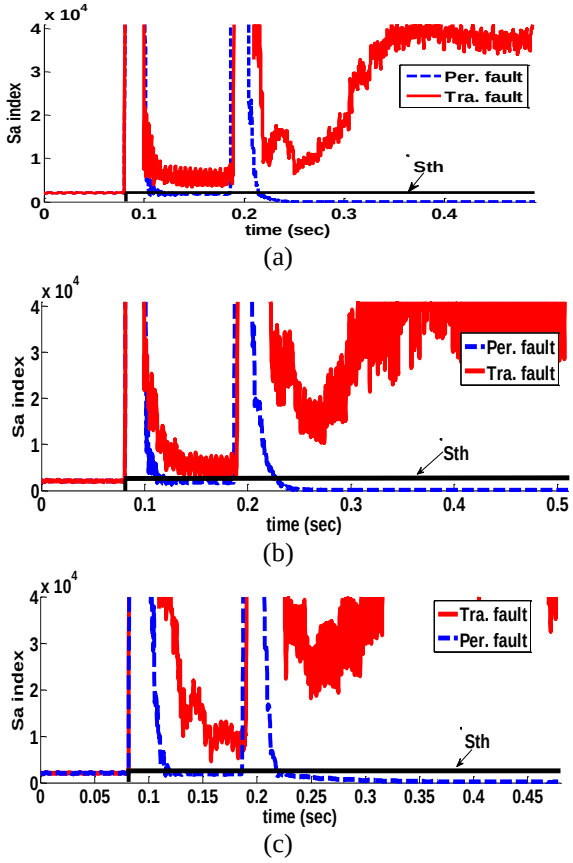

Fig. 9. *Behavior of index "S_a" under transient and permanent faults case 4 at different arc models at 160 Km from relay*
(a) For Arc1, **(b)** For Arc2, **(c)** For Arc3

Figure 10 shows the behaviour of the presented scheme under various sampling frequency (3.2 kHz and 6.4 kHz). Therefore, the accuracy of the presented scheme is independent of sampling frequency. But, it is very important to note that the sampling rate should equal at least 1.6 kHz, which means that the resolution level that will be reached is equal to the 5th level to determine the proposed indices.

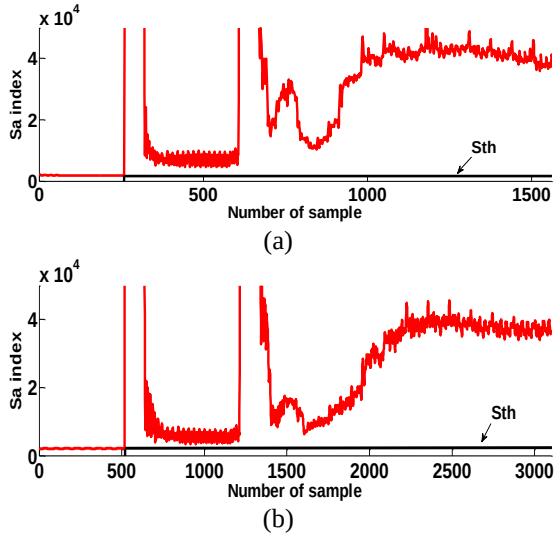

Fig. 10. *The proposed scheme behaviour under various sampling frequency*
(a) f_s= 3.2 kHz (64 samples /cycle) at 150 Km, **(b)** f_s= 6.4kHz (128 samples /cycle) at 150 Km

Under case 6, the presented scheme response is compared with the schemes illustrated in [5] and [7] for case 1. In Figures 11(a) and 11(b), the comparisons are depended on time delay in reclosing trip signal for various fault locations and pre-fault load angles, respectively. It provides the evidence that the presented algorithm has the fewest time delays.

To assess the fast response of the proposed scheme, Table 2 gives the total execution time for studied cases (Cases 1-4) at different fault locations and load angles, where T_{rec} and T_{que} are the reclosing command and the instant of the secondary arc quenching, respectively and $\boldsymbol{T_{exe}}$ equal to (T_{exe}=$T_{res} - T_{que}$). It is supposed that AG fault is on the TL at 0.1 s, and then at 0.2 s, the circuit breakers of the faulted phase are open from each end. From Table 2 and Figure 10, it is evident that the secondary arc extinction time is dependent on operating condition and fault position. Nevertheless, the proposed scheme will detect the instant of the arc extinction in around 10 ms in all cases.

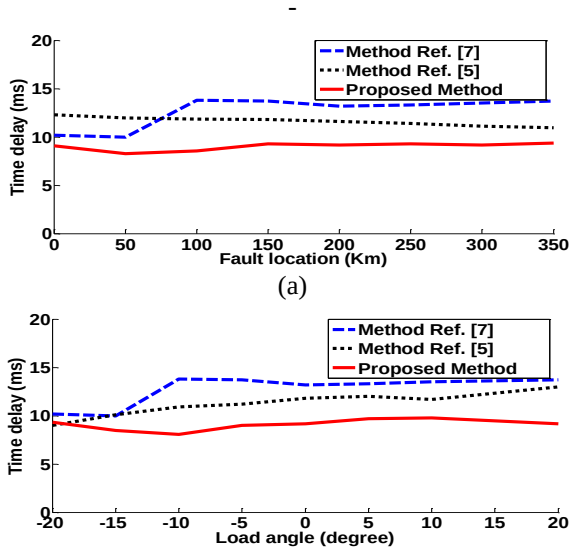

Fig. 11. *The proposed scheme behaviour under various sampling frequency*
(a) Fault location, **(b)** Load angle

4. Threshold Settings

The threshold value is adaptive in nature and is readjusted according to the load change and the status of a power system without any human interaction in order to alleviate the problem maintained in section II. Figure 12 shows the value of the threshold value with the load change for studied cases (Cases 1-5). It was shown from Figure 12 that the threshold value is changing adaptively to suite the changing loads and the status of a power system without any human interaction.

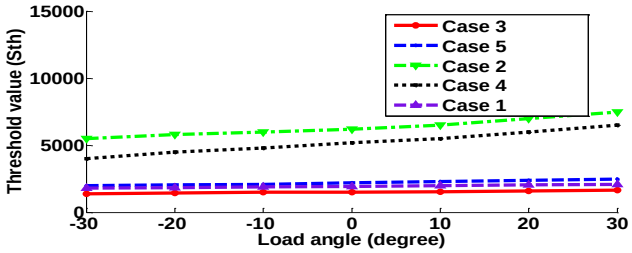

Fig. 12. *Behaviour of the threshold value (S_{th}) under different cases*

Table 2 Total execution time of studied cases

Cases	ARC type	Load angle (δ^o)	Fault location (km)	T_{que} (s)	T_{rec} (s)	T_{exe} (ms)
Case 1	Arc 1	-30	0	0.622	0.631	9.32
		-15	100	0.601	0.609	8.92
		0	180	0.635	0.643	8.43
		15	350	0.695	0.703	8.59
Case 2	Arc 1	-30	45	0.652	0.661	9.86
		-10	155	0.687	0.696	9.67
		0	240	0.601	0.610	9.58
		10	330	0.659	0.668	9.91
Case 3	Arc 1	-20	10	0.609	0.618	9.59
		-10	40	0.612	0.621	9.29
		0	90	0.598	0.607	9.35
		20	110	0.629	0.638	9.43
Case 4	Arc 2	-25	30	0.619	0.628	9.32
	Arc 2	-5	290	0.628	0.634	9.02
	Arc 3	0	50	0.631	0.640	9.82
	Arc 3	25	310	0.662	0.671	9.76

5. Comparison with Existing Scheme

Table 3 introduces a comparative summary among the close schemes and the proposed scheme. In the following section, a simulation based proof of the superiority of the proposed method is provided.

The authors in [8] and [13] used the third harmonic for both zero-sequence voltage and faulted phase voltage to determine the instant of the arc extinction; these two schemes are tested under the same condition. The classification rate was an appropriate gauge to examine the powerfulness of detection schemes which have been introduced in Figure 13, where third harmonic has a value under reactor compensation exists and this means that there is no arc extinction.

The advantages of the presented scheme compared to prior schemes are summarized as follow:

- The scheme estimates the instant of the arc quenching faster than other conventional schemes.
- The proposed scheme depends on an adaptive threshold level. It is set according to the feature of the circuits.
- Simple identification criterion and no need to sample current waveforms.

Table 3 ASPRS schemes compared to the proposed scheme

Item ======= Technique	Comm./ Non Comm.	Existence of Reactors	Existence of Capacitors	S/D	f_s (kHz)	Setting Threshold	Max detection time of arc extinction (ms)
FFT [6]	Non	NR	NR	Single circuit	6.4	Fixed	45
DFT [8]	Non	Fail detect time of secondary arc extinction	NR	Single circuit	NR	Adaptive	10
WPT [10]	Non		NR	Single circuit	10	No need	NR
WPT [11]	Non		NR	Double circuit	20	No need	NR
DFT [13]	Non		NR	Single circuit	NR	No need	NR
Calculated indices [9]	Communication	Success	NR	Single circuit	>0.72	Fixed	15
WPEE [12]	Non	NR	NR	Single circuit	20	Fixed	20
DFT [14]	Non	Success	NR	Double circuit	NR	Fixed	20
WPT [17]	Non	Success	NR	Successful	6.4	Adaptive	10
WPT [18]	Non	Success	NR	Successful	6.4	Adaptive	10
Proposed technique	Non	Success	Success	Successful	6.4	Adaptive	10

*NR = Not Reported
*f_s = Sampling frequency
*S/D = Single / Double circuit Application

6. Conclusion

This paper proposes the adaptive single poling autoreclosure adequate to the probable network-topology change. The proposed method uses the change in different order harmonics and DC component in order to discriminate the fault nature and identify the arc extinction instant under existing temporary fault, respectively. The selected harmonics and the DC component are extracted using WPT. The results proved that the presented method is able to distinguish the fault type and obtain the arc extinction instant via validation the method under several critical cases such as different arc models, different compensation element (shunt and series), and different network configurations. Also, the response of the presented technique is checked under various voltage levels like 400 kV (the simulated single circuit) and 500 kV (the simulated double circuit). The proposed scheme needs low sample frequency compared with other reported methods. Further, the extinction instant of the arc resulting from temporary faults is obtained in 10ms after extinguishing the simulated arc by ATP/EMTP. The obtained time is lower than that of some the reported methods and is equal to other ones.

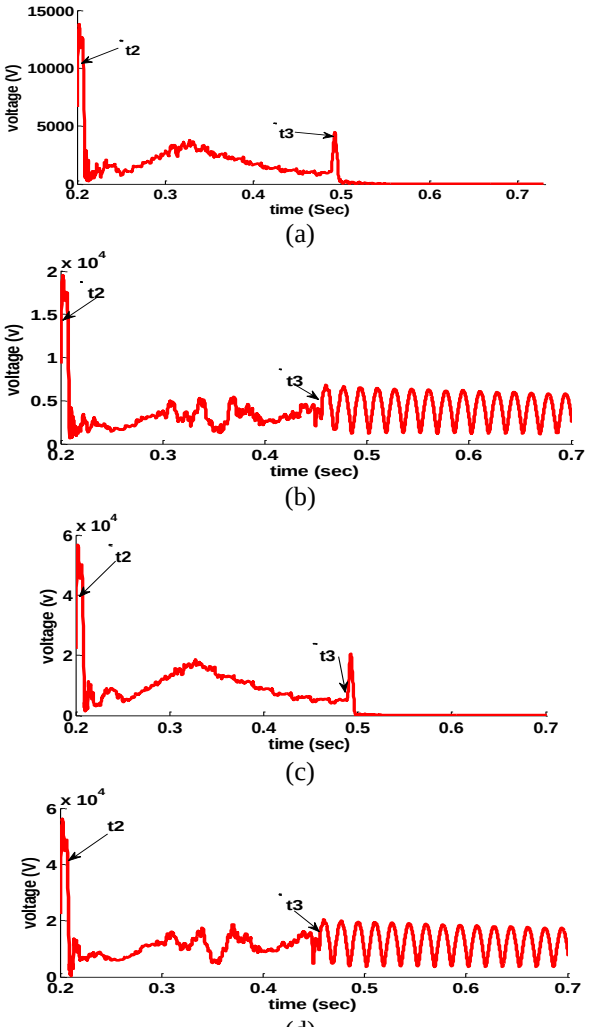

Fig. 13. *Third harmonic amplitude of zero-sequence voltage (a & b) as in Ref. [13] and third harmonic amplitude of faulted phase voltage (c & d) as in Ref. [8].*
(a) with reactor absence, **(b)** with reactor existence, **(c)** with reactor absence, **(d)** with reactor existence

7. References

[1] A. Rahmati and R. Adhami, “A Fault Detection and Classification Technique Based on Sequential Components”, IEEE Trans. on Industry Applications, 2014, 50, pp. 4202 – 4209.

[2] A. R. Adly, R. A. El Sehiemy and A. Y. Abdelaziz, “A Negative Sequence Superimposed Pilot Protection Technique during Single Pole Tripping”, Electric Power Systems Research, 2016, 137, pp. 175-189.

[3] K. Ngamsanroaj and S. Premrudeepreechacharn and N. R. Watson, “500 kV Single Phase Reclosing Evaluation Using Simplified Arc Model”, Emerging Technology and Advanced Engineering, 2004, 4 (6).

[4] A. R. Adly, R. A. El Sehiemy, A. Y. Abdelaziz and N. M. A. Ayad, “Critical Aspects on Wavelet Transforms Based Fault Identification Procedures in HV Transmission Line”, IET generation transmission & distribution, 2016, 10, pp. 508-517.

[5] N. I. Elkalashy, H. A. Darwish, A. M. I. Taalab and M. A. Izzularab“An adaptive single pole autoreclosure based on zero sequence power”, Electric Power Systems Research, 2007, 77, pp. 438– 446.

[6] H. M. Naimi, S. Hasanzadeh and M. S. Pasand, “Discrimination of arcing faults on overhead transmission lines for single-pole auto-reclosure”, European Trans. on Electrical Power, 2103, 23, pp. 1523–1535.

[7] S. P. Ah, C. H. Kim, R. K. Aggarwal, and A. T., “An alternative approach to adaptive single pole auto-reclosing in high voltage transmission systems based on variable dead time control,” IEEE Trans. Power Delivery, 2001, 16, pp. 676–686.

[8] S. Jamali and A. Parham, “New approach to adaptive single pole auto-reclosing of power transmission lines”, IET Generation, Transmission & Distribution, 2010, 4, pp. 115 – 122.

[9] H. K. Zadeh and Z. Li, “Design of a novel phasor measurement unit-based transmission line auto reclosing scheme”, IET Generation, Transmission & Distribution, 2011, 5, pp. 806–813.

[10] S. Jamali and N. Ghaffarzadeh, “Adaptive Single-pole Auto-reclosure for Transmission Lines Using Sound Phases Currents and Wavelet Packet Transform”, Electric Power Components and Systems, 2010, 38, pp. 1558-1576.

[11] S. Jamali and Ghaffarzadeh, “A wavelet packet based method for adaptive single-pole auto-reclosing”, Zhejiang University-SCIENCE (Computers & Electronics), 2010, 11, pp. 1016-1024.

[12] Y. Zhang, Q. Gong and X. Shi, “A Novel Adaptive Reclosure Criterion for HV Transmission Lines Based on Wavelet Packet Energy Entropy”, Advances in Neural Networks, 2009, 1, pp. 874 – 881.

[13] Z. M. Radojevi, “Numerical Algorithm for Adaptive Single Pole Autoreclosure Based on Determining the Secondary Arc Extinction Time”, Electric Power Components and Systems, 2006, 34, pp. 739-745.

[14] M. E. H. Golshan, and N. Golbon, “Detecting secondary arc extinction time by analyzing low frequency components of faulted phase voltage or sound phase current waveforms,” J. Elect. Eng., 2006, 88, pp.141–148.

[15] Z. Radojevi, and J. Shin, “New digital algorithm for adaptive re-closing based on the calculation of the faulted phase voltage total harmonic distortion factor,” IEEE Trans. Power Delivery, 2007, 22, pp.37–41.

[16] F. Zhalefar, M. D. Zadeh, and T. A. Sidhu, “High-speed adaptive single-phase reclosing technique based on local voltage phasors,” IEEE Trans. Power Delivery, 2015, PP, pp. 1–9.

[17] Ahmed R. Adly, Ragab A. El-Sehiemy, Almoataz Y. Abdelaziz, and Said A. Kotb. "An Accurate Technique for Discrimination between Transient and Permanent Faults in Transmission Networks." Electric Power Components and Systems, 2017, 45(4), pp. 366-381.

[18] Ahmed R. Adly, Ragab A. El Sehiemy, and Almoataz Y. Abdelaziz. "An integrated reclosing technique for enhancing transient stability under single pole tripping." In Power Systems Conference (MEPCON), 2016 Eighteenth International Middle East, 2016, pp. 67-72.

[19] F. D. Zahlay, K. S. Rama Rao and T. B. Ibrahim, “A New Intelligent Autoreclosing Scheme Using Artificial Neural Network and Taguchi’s Methodology”, IEEE Trans. on Industry Applications, 2010, 47, pp. 306 – 313.

[20] J. Barros, and R. I. Diego, “Analysis of Harmonics in Power System Using the Wavelet Packet Transform”, IEEE Trans. on Instrumentation and Measurement, 2008, 57, pp. 63 – 69.

[21] S. F. Huang and X. G. Wang, “A Fault Location Scheme Based on Spectrum Characteristic of Fault Generated High Frequency Transient Signals”, in Proc. IEEE Power & Energy Society General Meeting, 2009 , pp. 1-5,

[22] P. Jena A. K. and Pradhan, “Directional relaying during single-pole tripping using phase change in negative-sequence current. Power Delivery”, IEEE Trans. on Power Delivery, 2013, 28, pp.1548-1557.

[23] A. T. Johns, R. K. Aggarwal and Y. Song, “Improved technique for modeling fault arcs on faulted EHV transmission systems”, IET Generation, Transmission & Distribution, 1994, 141, pp. 148-154,.

[24] Y. Goda, M. Iwata, K. Keda, and S. Tanaka, “Arc voltage characteristics of high current fault arcs in long gaps”, IEEE Trans. Power Delivery, 2000, 15, pp. 791–795.

[25] B. Li, Y. L. Li, K. Sheng and Z. A. Zeng, “The study on single-pole adaptive reclosure of EHV transmission lines with the shunt reactor”, in Proc. CSEE, 2004 , pp. 52-56.